Table III. Carboxylate-Zinc Interactions

enzyme	ligand	distance, Å O1-Zn	distance, Å O2-Zn	coord stereochem	ref
CPA	Bz-Phe	2.7	2.2	syn	18
CPA	"potato" inhibitor	3.2	1.8	syn	36
TLN	*N*-(1-carboxy-3-phenylpropyl)Leu-Trp	2.4	2.0	syn	23
TLN	Cbz-Phe	3.0	2.1	syn	26
TLN	benzylsuccinate	4.1	2.1	anti	21

demands of the rest of the benzylsuccinate inhibitor require a nonoptimal anion-cation interaction. The geometries of carboxylate-zinc interactions as observed in CPA and TLN are compared in Table III.

Summary

The phosphonamidate ZGP′ binds to CPA as an analogue of a possible intermediate or transition state along a promoted-water hydrolytic pathway. The tetrahedral phosphonamidate moiety, which straddles the active site zinc ion, is oriented differently when compared to the tetrahedral *gem*-diol(ate) CPA inhibitors[12,15,17,19] or related TLN-phosphon(amid)ate complexes[24,25] recently reported. This may be due to the fact that ZGP′ displays an anomalous binding mode to CPA where the Cbz-Gly portion of the inhibitor occupies the hydrophobic cleft normally occupied by the side chains of P_1 amino acids or analogues thereof.[18,19,36] This alternative strong binding mode may bear some relevance to general phenomena involving slow-binding enzyme inhibitors, as has been demonstrated for phosphonamidates that bind to TLN.[25] When anionic inhibition of CPA and TLN by phosphon(amid)ates is compared with that of related carboxylate-derived compounds, it is seen that zinc-carboxylate interactions prefer syn-coordinated carboxylates. This coordination appears to tend toward bidentate if no overriding steric factors persist. This stereochemical feature is important in the design of inhibitors derived from carboxylates and phosphon(amid)ates targeted toward those zinc proteases of known and unknown structure.

Acknowledgment. We thank Prof. Paul A. Bartlett (University of California, Berkeley) for the generous gift of ZGP′. Additionally, we thank Prof. Richard E. Galardy for many helpful discussions, and we thank Dr. Alfonso Mondragon for his assistance with the figures. Finally, we are grateful to the National Institutes of Health for Grant GM 06920 in support of this research.

Communications to the Editor

Simultaneous Observation of O-O and Fe-O_2 Stretching Vibrations of Fe(TPP)O_2 in Dioxygen Matrices by Resonance Raman Spectroscopy

Wolf-Dieter Wagner, Insook Rhee Paeng, and
Kazuo Nakamoto*

Todd Wehr Chemistry Building
Marquette University, Milwaukee, Wisconsin 53233

Received April 4, 1988

The observation of $\nu(O_2)$ and $\nu(Fe-O_2)$ (ν: stretching) vibrations of oxyiron porphyrins is highly important in elucidating the nature of the O-O and Fe-O_2 bonds in oxygen transport/storage proteins such as hemoglobin (Hb) and myoglobin (Mb). Although Caughey and co-workers[1-4] observed the $\nu(O_2)$ of HbO_2 and MbO_2 at ~1155, ~1130, and ~1105 cm^{-1} in IR spectra, the corresponding $\nu(Fe-O_2)$ vibrations have not been observed by IR spectroscopy. On the other hand, attempts to observe the $\nu(O_2)$ of these heme proteins by resonance Raman (RR) spectroscopy have been unsuccessful although the $\nu(Fe-O_2)$ of HbO_2 was readily observed at 567 cm^{-1} by Soret excitation.[5] Different from oxyiron porphyrins, the $\nu(O_2)$ and $\nu(Co-O_2)$ of oxycobalt porphyrins can be resonance-enhanced simultaneously, and extensive RR studies have already been carried out on Co(II)-substituted heme proteins[6,7] and their model compounds.[8,9] Thus far, RR observation of the $\nu(O_2)$ of oxyiron porphyrins has been successful only for those containing axial thiolate ligands[10,11] although the reason for this is not clear. In this communication, we report the first

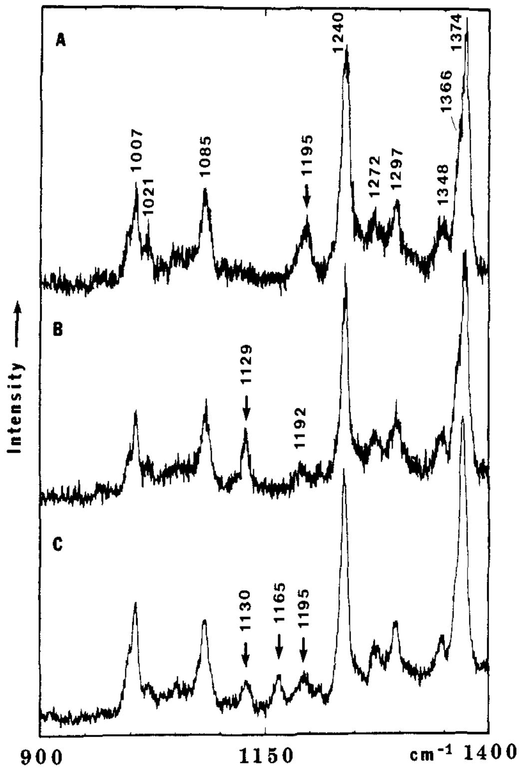

Figure 1. RR spectra (high frequency region) of cocondensation products of Fe(TPP) with (A) $^{16}O_2$, (B) $^{18}O_2$, and (C) scrambled dioxygen ($^{16}O_2$/$^{16}O^{18}O$/$^{18}O_2$ in an ca. 1:2:1 ratio) at ~25 K (406.7-nm excitation).

---

(1) Barlow, C. H.; Maxwell, J. C.; Wallace, W. J.; Caughey, W. S. *Biochem. Biophys. Res. Commun.* **1973**, *55*, 91-95.

(2) Maxwell, J. C.; Volpe, J. A.; Barlow, C. H.; Caughey, W. S. *Biochem. Biophys. Res. Commun.* **1974**, *58*, 166-171.

(3) Caughey, W. S.; Choc, M. G.; Houtchens, R. A. "Bonding and Reactions of Dioxygen Bound to Hemeproteins" In *Biochemical and Clinical Aspects of Oxygen*; Caughey, W. S., Ed.; Academic Press: New York, 1978; pp 1-18.

(4) Potter, W. T.; Tucker, M. P.; Houtchens, R. A.; Caughey, W. S. *Biochemistry* **1987**, *26*, 4699-4707.

(5) Brunner, H. *Naturwissenschaften* **1974**, *61*, 129.

(6) Tubaki, M.; Yu, N.-T. *Proc. Natl. Acad. Sci. U.S.A.* **1981**, *78*, 3581-3585.

(7) Mackin, H. C.; Tsubaki, M.; Yu, N.-T. *Biophys. J.* **1983**, *41*, 349-357.

(8) Bajdor, K.; Kincaid, J. R.; Nakamoto, K. *J. Am. Chem. Soc.* **1984**, *106*, 7741-7747.

(9) Bajdor, K.; Nakamoto, K.; Kanatomi, H.; Murase, I. *Inorg. Chim. Acta* **1984**, *82*, 207-210.

(10) Chottard, G.; Schappacher, M.; Ricard, L.; Weiss, R. *Inorg. Chem.* **1984**, *23*, 4557-4561.

(11) Bangcharoenpaurpong, O.; Rizos, A. K.; Champion, P. M.; Jollie, D.; Sliger, S. G. *J. Biol. Chem.* **1986**, *261*, 8089-8092.

0002-7863/88/1510-5565$01.50/0

simultaneous observation of the $\nu(O_2)$ and $\nu(Fe{-}O_2)$ vibrations of $Fe(TPP)O_2$ (TPP: tetraphenylporphyrinato anion) in O_2 matrices by RR spectroscopy.

The samples of $Fe(TPP)O_2$ in O_2 matrices were prepared by using the laser beam heated miniature oven techniques reported previously.[12,13] RR spectra were obtained by using the 406.7-nm line of a Coherent Innova-100-K3 Kr-ion laser. A backscattering arrangement was set up with a cylindrical lens to produce a line focus on the sample surface. Scattered light was analyzed with a Spex Model 1403 double monochromator coupled with a Hamamatsu R 928 photomultiplier and a Spex DM1B computer.

Figure 1 shows the RR spectra of $Fe(TPP)O_2$ in O_2 matrices at ~25 K. Traces A, B, and C were obtained by using $^{16}O_2$, $^{18}O_2$, and scrambled O_2 (a mixture of $^{16}O_2$, $^{16}O^{18}O$, and $^{18}O_2$ in an approximately 1:2:1 ratio), respectively. The band at 1195 cm^{-1} (trace A) is shifted to 1129 cm^{-1} by $^{16}O_2/^{18}O_2$ substitution (trace B). The observed shift is in perfect agreement with the theoretical value expected for a diatomic O–O vibrator. Furthermore, the scrambled dioxygen matrix (trace C) exhibits an additional band due to the $^{16}O^{18}O$ adduct at 1165 cm^{-1} located between those of the $^{16}O_2$ and the $^{18}O_2$ adducts. The fact that the intensity pattern of the $\nu(O_2)$ bands does not exactly match the expected 1:2:1 ratio may be attributed to the presence of small underlying porphyrin bands near 1192 and 1129 cm^{-1}. Previously, we[14] observed the $\nu(O_2)$ of $Fe(TPP)O_2$ in O_2/Ar matrices by using IR spectroscopy. In that case, we observed two oxygen-isotope sensitive bands at 1195 and 1106 cm^{-1} for $Fe(TPP)^{16}O_2$ and assigned them to the "end-on" and "side-on" type dioxygen adducts, respectively. The RR frequencies obtained above are in excellent agreement with those of the "end-on" adducts observed in IR spectra. Theoretically, the $\nu(^{16}O^{18}O)$ band of the "end-on" adduct should split into two peaks due to the mixing of the $Fe{-}^{16}O^{18}O$ and $Fe{-}^{18}O^{16}O$ adducts. As shown in our previous work,[14] this splitting is too small to be observed under our experimental conditions. Although the $\nu(O_2)$ of the "side-on" adducts were not observed in RR spectra, this may be attributed to their low concentration relative to the "end-on" adducts.[14] The oxidation/spin state (ν_4) and spin state/core size (ν_2) marker bands[15-17] of $Fe(TPP)O_2$ are located at 1366 and 1558 cm^{-1}, respectively, close to the analogous frequencies of $Fe^{III}(TPP)X$ with ($X = Cl^-, N_3^-$)[15,18] or $Fe^{III}(T_{piv}PP)Br$.[15] Thus, the "end-on" adduct can be regarded as a five-coordinated Fe(III) high spin complex approximated by the $Fe^{III}(TPP)O_2^-$ formulation.

Figure 2 shows the low-frequency RR spectra of $Fe(TPP)O_2$ which correspond to those shown in Figure 1. It is seen that the bands at 853 and 509 cm^{-1} (trace A) are shifted to 819 and 487 cm^{-1} (trace B), respectively, by $^{16}O_2/^{18}O_2$ substitution and that the scrambled dioxygen matrix exhibits both of these bands with almost equal intensities. (The porphyrin band at 816 cm^{-1} (trace A) is hidden under the strong band at 819 cm^{-1} in traces B and C.) The bands at 853 and 819 cm^{-1} have already been assigned to the $\nu(Fe{=}O)$ of ferrylporphyrin, OFe(TPP), and its ^{18}O analogue, respectively, which were produced by laser photolysis of the respective dioxygen adducts.[13,19] The bands at 509 and 487 cm^{-1} were observed for the first time and are assigned to the $\nu(Fe{-}O_2)$ of $Fe(TPP)O_2$ and its $^{18}O_2$ analogue, respectively, in accordance with the expected isotopic shift. These frequencies are considerably lower than the $\nu(Fe{-}O_2)$ of six-coordinate complexes due to the lack of electron donation from the base to dioxygen. For example, the $\nu(Fe{-}O_2)$ of $Fe(TPP)(piperidine)O_2$ and its $^{18}O_2$ derivative are at 575 and 551 cm^{-1}, respectively.[20] As shown previously,[21] the $\nu(Fe{-}^{16}O^{18}O)$ and $\nu(Fe{-}^{18}O^{16}O)$ are very close to the $\nu(Fe{-}^{16}O^{16}O)$ and $\nu(Fe{-}^{18}O^{18}O)$, respectively. Therefore, only two $\nu(Fe{-}O_2)$ bands are expected in case of scrambled dioxygen. As the laser power is increased or the irradiation time is lengthened, the $\nu(Fe{=}O)$ at 853 cm^{-1} becomes stronger, and the $\nu(O_2)$ at 1195 cm^{-1} and the $\nu(Fe{-}O_2)$ at 509 cm^{-1} become weaker thus supporting our proposal[13,19] that OFe(TPP) is formed via the following steps

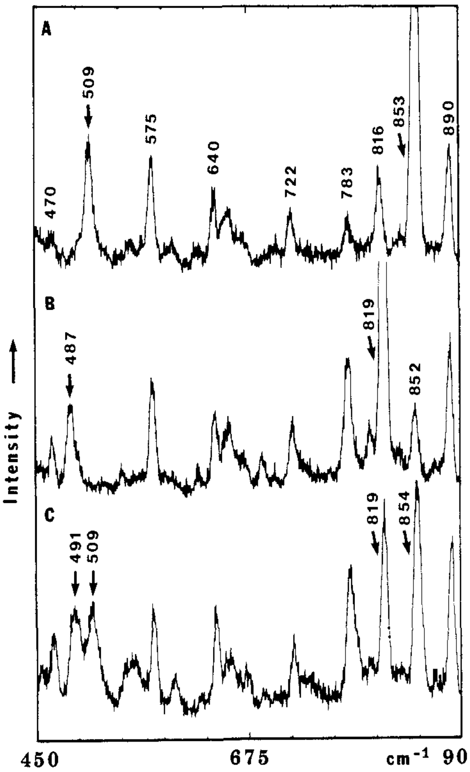

Figure 2. RR spectra (low-frequency region) of cocondensation products of Fe(TPP) with (A) $^{16}O_2$, (B) $^{18}O_2$, and (C) scrambled dioxygen ($^{16}O_2/^{16}O^{18}O/^{18}O_2$ in an ca. 1:2:1 ratio) at ~25 K (406.7-nm excitation).

$$Fe(TPP) + O_2 \rightarrow Fe(TPP)O_2 \xrightarrow{h\nu} OFe(TPP) + {}^1/_2O_2$$

This should be contrasted to the results of our RR studies on oxidation of Fe(TMP) (TMP: tetramesitylporphinato anion) in toluene solution at low temperatures.[22] In that case, OFe(TMP) was formed via the cleavage of the Fe–O–O–Fe bond of the dimeric species

$$Fe(TMP) + O_2 \rightarrow Fe(TMP)O_2 \xrightarrow{Fe(TMP)} (TMP)Fe{-}O{-}O{-}Fe(TMP) \xrightarrow{\Delta} 2\,O{=}Fe(TMP)$$

We have located the $\nu(Fe{=}O)$ of OFe(TMP) and the $\nu_{sym}(Fe{-}O)$ of the bridging species at 845 and 574 cm^{-1}, respectively, at ~195 K and noted that the former becomes stronger and the latter disappears completely when the temperature is raised to ~227 K.

It has been tacitly assumed that the failure to resonance-enhance the $\nu(O_2)$ of oxyiron porphyrins is either due to the absence of the $Fe{-}O_2$ CT transition in the 400–700-nm region[23] or to its small oscillator strength. These assumptions must be reexamined in the light of the present results.

---

(12) Scheuermann, W.; Nakamoto, K. *Appl. Spectrosc.* **1978**, *32*, 251–252.

(13) Proniewicz, L. M.; Bajdor, K.; Nakamoto, K. *J. Phys. Chem.* **1986**, *90*, 1760–1766.

(14) Watanabe, T.; Ama, T.; Nakamoto, K. *J. Phys. Chem.* **1984**, *88*, 440–445.

(15) Burke, J. M.; Kincaid, J. R.; Peters, S.; Gagne, R. R.; Collman, J. P.; Spiro, T. G. *J. Am. Chem. Soc.* **1978**, *100*, 6083–6088.

(16) Stong, J. D.; Spiro, T. G.; Kubaska, R. J.; Shupack, S. I. *J. Raman Spectrosc.* **1980**, *9*, 312–314.

(17) Chottard, G.; Battioni, P.; Battioni, J.-P; Lange, M.; Mansuy, D. *Inorg. Chem.* **1981**, *20*, 1718–1722.

(18) Wagner, W.-D.; Nakamoto, K., to be published.

(19) Bajdor, K.; Nakamoto, K. *J. Am. Chem. Soc.* **1984**, *106*, 3045–3046.

(20) Nakamoto, K.; Paeng, I. R.; Kuroi, T.; Isobe, T.; Oshio, H. *J. Mol. Struct.*, in press.

(21) Duff, L. L.; Appelman, E. H.; Shriver, D. F.; Klotz, I. M. *Biochem. Biophys. Res. Commun.* **1979**, *90*, 1098–1103.

(22) Paeng, I. R.; Shiwaku, H.; Nakamoto, K. *J. Am. Chem. Soc.* **1988**, *110*, 1995–1996.

(23) Case, D. A.; Huynh, B. H.; Karplus, M. *J. Am. Chem. Soc.* **1979**, *101*, 4433–4453.

Acknowledgment. This work was supported by the National Science Foundation (DMB-8613741). W.-D.W. is a recipient of a Feodor Lynen Fellowship from the Alexander von Humboldt Foundation. We thank L. Proniewicz for stimulating discussions.

Registry No. Fe(TPP)O_2, 88083-22-1; O_2, 7782-44-7; OFe(TPP), 84152-32-9; ^{18}O, 14797-71-8.

Synthesis of 2-Functionalized 1,1-Diiodo-1-alkenes. Generation and Reactions of 1-Iodo-1-lithio-1-alkenes and 1,1-Dilithio-1-alkenes

José Barluenga,* Miguel A. Rodríguez, and Pedro J. Campos

Departamento de Química Organometálica
Universidad de Oviedo, 33071-Oviedo, Spain

Gregorio Asensio

Departamento de Química Orgánica
Universidad de Valencia, 46010-Valencia, Spain

Received December 9, 1987
Revised Manuscript Received May 19, 1988

In recent years, 1,1-dilithio-1-alkenes have been the center of interest.[1,2] A few compounds of this class have been prepared,[1,3] but in all the cases the 1,1-dilithioalkenes were unfunctionalized. We report here the first preparation of a β-functionalized 1,1-dilithio-1-alkene and its precursor, a 1-iodo-1-lithio-1-alkene, by treatment of a 1,1-diiodo-1-alkene with organolithium compounds as well as some synthetic applications of these lithioalkenes. A general method for the synthesis of previously undescribed 2-substituted 1,1-diiodo-1-alkenes are also shown.

Examples of 1,1-diiodo-1-alkenes containing a function in 2-position are unknown,[4] but they could be appropriate antecedents for functionalized 1,1-dilithio-1-alkenes. This fact prompted us to study the reactivity of 1-iodoacetylenes **1**[5] toward bis(pyridine)iodine(I) tetrafluoroborate **2**,[6] since this reagent adds I^+Nu^- to internal acetylenes[7] and thus would lead to a general entry to 1,1-diiodo-1-alkenes **3**.

When the iodinating reagent **2** is allowed to react with 1-iodoacetylenes **1** and a wide variety of nucleophiles **4**, 2-substituted 1,1-diiodo-1-alkenes **3** are produced in good to very good yields (see eq 1 and Table I).

$$\underset{\mathbf{1}}{R\text{-}C{\equiv}C\text{-}I} + \underset{\mathbf{2}}{I(py)_2.BF_4} + \underset{\mathbf{4}}{Nu(NuH)} \longrightarrow \underset{\mathbf{3}}{(R)(Nu)C{=}CI_2} \quad (1)$$

1a, R = Ph; **1b**, R = n-C_4H_9

The reaction conditions are similar to the additions earlier mentioned.[7] These processes are clean, and, after the usual workup procedures, compounds **3** are obtained in more then 90% purity.

Table I. Synthesis of Compounds **3**

1	nucleophile	solvent	time[a] (h)	3	yield[b] (%)
a	$ClSiMe_3$	CH_2Cl_2	3	**a**[c]	65
a	Br^-	$MeCN/H_2O$	60	**b**	64
b	I^-	MeOH	14	**c**	70
a	NCS^-	dioxane/H_2O	60	**d**	75
a	pyridine	CH_2Cl_2	20	**e**	57
b	CH_3COOH	CH_3COOH/CH_2Cl_2 (2:1)	14	**f**	63
a	HCOOH	85% $HCOOH/CH_2Cl_2$ (2:1)	14	**g**	85
a	i-PrOH	i-PrOH/CH_2Cl_2 (2:1)	4	**h**	80
a	anisole	CH_2Cl_2	22	**i**[d]	50[e]
a	PhSH	CH_2Cl_2	15	**j**	80

[a] At room temperature except for the synthesis of **3a** and **3i** (−50 °C). [b] Yields of isolated products, relative to starting **2** and not optimized. [c] Structural formula (Ph)(Cl)C=CI_2. [d] Structural formula (Ph)(p-$CH_3OC_6H_4$)C=CI_2. [e] The crude reaction mixture contains 20% of p-iodoanisole.

Scheme I

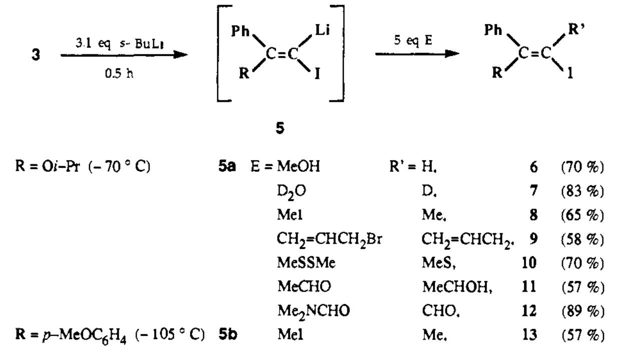

Scheme II

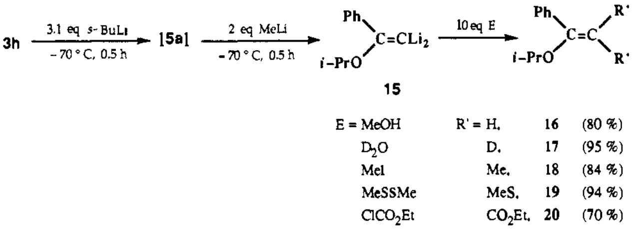

The synthetic potential of these new 2-functionalized 1,1-diiodo-1-alkenes by transformation of each iodine atoms is noteworthy. In this paper we describe the conversion of aromatic 1,1-diiodo-1-alkenes **3** to 1-iodo-1-alkenes and 1,1-dilithio-1-alkenes.

When compound **3** bearing an isopropoxy (**3h**) or a p-methoxyphenyl (**3i**) group in the 2-position is treated in THF with an excess of *sec*-butyllithium, a solution of the organolithium system **5** is obtained. The reaction of **5** with different electrophiles gives the corresponding monosubstituted products **6–13** (Scheme I).

The solution of **5a** is stable at −20 °C. Above this temperature it slowly begins to decompose, yielding the product **6** corresponding to abstraction of a solvent proton. At room temperature treatment of **5a** with an excess of iodomethane gives a complex mixture of **8**, **6**, and 1-isopropoxy-2-phenylacetylene (analyzed by ^{13}C NMR).

A solution of **5a** in the presence of cuprous chloride (3 equivs) at −60 °C is quantitatively transformed in 1,4-diisopropoxy-1,4-diphenyl-1,2,3-butatriene (**14**)[8] in 2 h (eq 2).

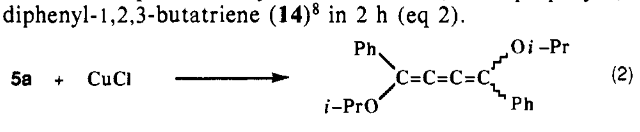

14

---

(1) Maercker, A.; Theis, M. *Top. Curr. Chem.* **1987**, *138*, 1–61.

(2) Apeloig, Y.; Schleyer, P. R.; Binkley, J. S.; Pople, J. A. *J. Am. Chem. Soc.* **1976**, *98*, 4332–4334. Nagase, S.; Morokuma, K. *J. Am. Chem. Soc.* **1978**, *100*, 1661–1666. Laiding, W. D.; Schaefer, H. F. *J. Am. Chem. Soc.* **1979**, *101*, 7184–7188.

(3) Morrison, J. A.; Chung, C.; Lagow, R. J. *J. Am. Chem. Soc.* **1975**, *97*, 5015–5017. Maercker, A.; Dujardin, R. *Angew. Chem., Int. Ed. Engl.* **1984**, *23*, 224. Maercker, A.; Dujardin, R. *Angew. Chem., Int. Ed. Engl.* **1985**, *24*, 571–572.

(4) Gaviña, F.; Luis, S. V.; Ferrer, P.; Costero, A. M.; Marco, J. A. *J. Chem. Soc., Chem. Commun.* **1985**, 296–297.

(5) Barluenga, J.; González, J. M.; Rodríguez, M. A.; Campos, P. J.; Asensio, G. *Synthesis* **1987**, 661–662.

(6) Barluenga, J.; González, J. M.; Campos, P. J.; Asensio, G. *Angew. Chem., Int. Ed. Engl.* **1985**, *24*, 319–320.

(7) Barluenga, J.; Rodríguez, M. A.; González, J. M.; Campos, P. J.; Asensio, G. *Tetrahedron Lett.* **1986**, *27*, 3303–3306.

(8) Compound **14** is a stable yellow solid (mp 105–107 °C, MeOH) corresponding to a single diastereoisomer but at 60 °C in methanol is converted in a cis–trans mixture (1:1). Its spectral data (IR, ^1H and ^{13}C NMR, and MS) and the acidic hydrolysis to *trans*-1,4-diphenyl-2-buten-1,4-dione are in accordance with the proposed 1,2,3-butatrienic structure.

0002-7863/88/1510-5567$01.50/0